REFERENCE EVAPOTRANSPIRATION BORDERS MAPS OF EGYPT BASED ON KRIGING SPATIAL STATISTICS METHOD

Mohammed A. El-Shirbeny[*(1)], Bassam Abdellatif[(2)]

[*(1)] Agricultural applications department, NARSS, Egypt
[(2)] Digital Image Proc. and its App. department, NARSS, Egypt
23 Joseph Tito St. El-Nozha El-Gedida, Cairo, Egypt

ABSTRACT: The main idea of this research depends on defining and mapping the borders of minimum and maximum reference Evapotranspiration (*ETo*) on a spatial and temporal basis (over the period from 1979 to 2014 in every region in Egypt). Acceptable results could be achieved through using appropriate equation adjusted to local conditions to calculate *ETo*. These results should help the Egyptian government and policy makers to identify priorities for agricultural land reclamation, where the most important limiting factor in Egypt, for the agricultural sector, is water. Estimation of *ETo* according to FAO-Penman-Monteith (*FPM*) method depends on Location, Elevation, Temperature, solar radiation (sun shining hours), relative humidity (*RH*) and wind speed which are mandatory parameters to calculate *ETo*. Although the scarcity of climate data is a major problem in most developing countries, the climatic mathematical models are considered as the best solution for none or rare climatic database regions. These models depend on many parameters which can be derived from the remotely sensed data. The modeled data must be evaluated and calibrated with a measured data. The modeled *Tmax*, *Tmin* and *Rad* were validated with measured data with R^2 as high as 0.97, 0.85 and 0.95 respectively. The R^2 between obtained *ETo* from measured data and the resulted *ETo* from modeled data was 0.9. The resulted linear equation was used to calibrate the results of *ETo* from modeled data. Kiriging-spatial-statistics method (*KSS*) was used to generate spatial surface maps of *ETo*. Monthly minimum, maximum and mean *ETo* maps were produced using *KSS* method.

Keywords: Modeled data, Agricultural planning, GIS, Water management and Arid climate.

1. INTRODUCTION

Egypt suffers from a relative shortage of water resources to population in terms of the per capita availability of water. The per capita availability of water in Egypt is less than 1,000 cubic meters since more than twenty years [1-3]
Agricultural sector consumes more than 80% of water resources. The agricultural land area was 3.3 *Mha* in summer, 2013 [4] and the population is 90 million people based on Dec. 2015 estimation. The agricultural area per capita is smaller than the lowest border of living (0.036 ha) and needs to be expanded horizontally and vertically in the next decades.
The dominant climate in Egypt has a direct impact on the consumption of water resources. Evapotranspiration (ET) is a good criterion to determine the range of water consumption as it reflects the actual consumption. The calculation of the amount of water consumed by ET is necessary for water management planning. If the ET model calculation is accurate, the planning of water management will be satisfactory [5-9].
ETo is a combination of Evaporation (*E*) and Transpiration (*T*). It represents the environmental demand for the sum of *E* and *T*. The *ETo* represented as short green grass in a case of 100% vegetation cover, and uniform height under non-water-stressed conditions. Under dry conditions, *ETo* is very significant for rationalization of irrigation water. In Egypt, the climate is hard where precipitation is rare, temperature and solar radiation is high [10]. Egypt suffers from the increasing of *ETo* rate by local dry climate, besides water resources scarcity and population increase [11-13].
There are many ways to calculate the *ETo,* based on a number of parameters in the equation. They were conducted by several amendments and calibrations to *ETo* calculation equations to suit different weather conditions of different regions in the world. For each prevalent climatic case, there is an equation suitable for use. In dry areas, which suffer from high temperature and radiation, Blaney-Criddle and Hargreaves methods are suitable. In humid areas, the suitable method is radiation method. The *FPM* method fits different climate conditions, because it depends on several factors, including; air temperature, solar radiation, wind speed and *RH* [14-17].

In this study, an attempt was made to help decision makers in Egypt to take the right decision to locate the agricultural reclamation areas based on the classification of water consumption as the biggest problem facing Egypt is the per capita water beside the per capita cultivated land. *ETo* maps will also support farmers to apply the right amount of water to their farms.

2. MATERIALS AND METHODS

2.1 The study area description

Egypt is located in the northern-east corner of Africa (fig., 1). A Digital Elevation Model (*DEM*) of Egypt, (fig., 2). Shows elevations ranged from about -400 up to about 2500 m(*A.S.L.*). It has a dry arid climate, where solar radiation is available all the year (Table, 1), precipitation is rare and *ET* is high [10]. Water resources are limited and facing many challenges in the present and in the future. The main water resource is the River Nile, which provides Egypt with 55.5 Km^3 of water yearly.
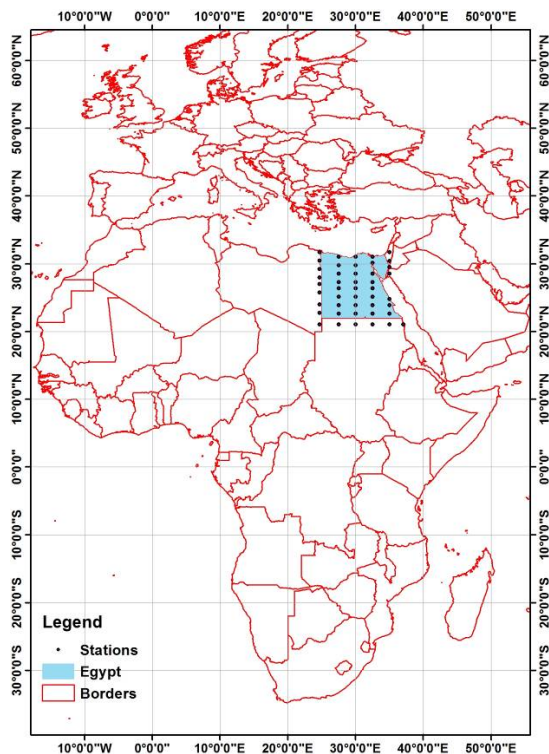

Fig. 1 The distinguished location of Egypt and distribution of modeled data weather stations

45 well-distributed modeled data stations (Table, 2) were used to calculate *ETo* based on *FPM* method. Alexandria (30 E and 31.1 N) and Toshka

(30 E and 21.1 N) ground stations were used to calibrate and validate the modeled data elements and *ETo* results.

2.2 FPM equation

FPM is the most common and spread method in the world. The equation uses standard climatological data of solar radiation (sunshine), air temperature, humidity and wind speed at 2 m above a surface area of green vegetation, shading the ground and well watered [14].

$$ETo = \frac{0.408\Delta(R_n - G) + \gamma \dfrac{900}{T + 273} u_2(e_s - e_a)}{\Delta + \gamma(1 + 0.34u_2)} \quad (1)$$

Where; *Rn*, net *Rad* [*MJ m^{-2} day^{-1}*], *G*, soil heat flux density [*MJ m^{-2} day^{-1}*], *T*, mean daily air temperature at 2 m height [°C], u_2, wind speed at 2 m height [*m s^{-1}*], e_s, saturation vapor pressure [*kPa*], e_a, actual vapour pressure [*kPa*], e_s -e_a, saturation vapor pressure deficit [*kPa*], Δ, slope vapour pressure curve [*kPa °C^{-1}*], γ, psychrometric constant [*kPa °C^{-1}*].
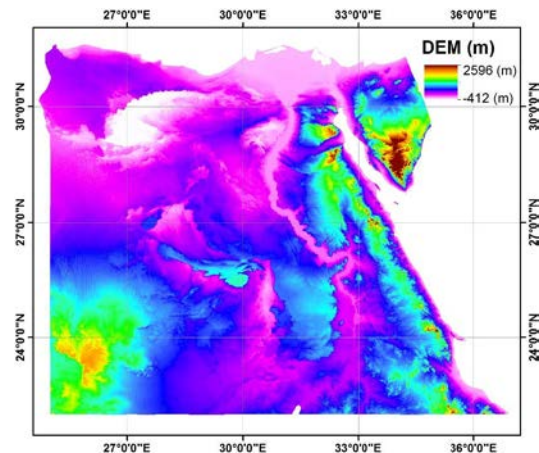

Fig. 2 Digital Elevation Model (DEM) of Egypt

2.3 Validation of modeled data

Alexandria and Toshka weather stations were used to validate the most effective weather elements (e.g. maximum air temperature (*Tmax*), minimum air temperature (*Tmin*) and solar radiation (*Rad*)). The relation between modeled and measured data was good, where R^2 was high as 0.97, 0.85 and 0.95 for *Tmax*, *Tmin* and *Rad* respectively. The *ETo* resulted from measured data used to validate the *ETo* resulted from modeled data and the R^2 was high as 0.9 (fig., 3). The resulted linear equation was used to calibrate the results of *ETo* from modeled data.

Table (1) monthly sun hours data for deferent locations in Egypt

Station	Jan	Feb	Mar	Apr	May	Jun	Jul	Aug	Sep	Oct	Nov	Dec
Sidi-Barrani	6 .9	7 .8	7 .9	9	10.8	12.2	12 .1	12 .1	10 .6	9 .2	8 .4	6 .8
Matrooh	6 .9	7 .8	7 .9	9	10.6	11.7	12 .1	11.9	10.5	8.9	8	6 .4
Alexandria	6 .4	7 .8	8.2	9.1	10.6	11.8	12 .0	11.3	10.3	9.6	7.3	6.2
Damitta	7.2	8.3	8.4	9.7	11.4	12.5	12.3	11.9	10.7	9.7	8.1	6.6
Port-Said	7	7.8	8.4	9.1	11.2	12.1	12.1	11.6	10.5	9.7	8	6.8
Al-Tahrir	7.4	7.9	8.8	9.8	11	12.2	12.2	11.8	10.6	9.6	7.8	7.2
Tanta	7.2	8.1	8.7	9.9	11	11.5	12	11.4	10.7	9.5	8.3	7.2
Bahtim	7	8 .3	8 .6	9.6	10.8	11.9	11.8	11.2	10.4	9.6	8.2	7.7
Almaza	7.6	7.8	8.6	8.9	11.2	11.9	11.4	11.4	9.5	9.4	8.2	7.6
El-Giza	7.8	8.2	8.8	9.6	11.2	12.2	12	11.5	10.5	9.8	8.5	7.7
Siwa	8.3	9.3	9.1	9.3	11.1	12.3	12.6	12	10.7	9.7	9.7	8
El-Kharga	9.1	9.7	10.2	10.4	11.5	12.2	12.4	12	11	10.6	9.9	9.5
Al-Minia	8.7	9.4	9.5	10.1	11.4	12.5	12.6	12	10.8	10.2	9.2	8.3
Hurghada	9.4	9.7	9.7	10.1	11.5	12.8	12.7	12.1	11.2	10.4	9.1	9.1
Aswan	9.4	9.2	9.4	10.6	11.8	12.4	12.3	11.6	10.9	10.5	9.6	9.6
Owainat	7.7	8.8	9.8	10.3	10.2	10	9.9	9.6	9.6	9.2	7.1	7.1

*After Muhammad Munir Mujahed, Energy sources in Egypt and the prospects of development, p.51 [19].

Table (2) the coordinates of modeled data stations.

NO	E	N	Z (m)	NO	E	N	Z (m)
1	25	21.1	645	24	32.5	26.4	467
2	27.5	21.1	405	25	25	27.0	209
3	30	21.1	311	26	27.5	27.3	239
4	32.5	21.1	606	27	30	27.3	164
5	35	21.1	634	28	32.5	27.3	613
6	37	21.1	254	29	25	27.9	144
7	27.5	22.6	424	30	27.5	28.6	51
8	30	22.6	183	31	30	28.6	128
9	32.5	22.6	173	32	32.5	28.6	470
10	35	22.6	716	33	35	28.6	532
11	25	23.3	552	34	25	29.2	28
12	25	23.9	512	35	35	29.5	164
13	27.5	23.9	450	36	27.5	29.8	-88
14	30	23.9	246	37	30	29.8	227
15	32.5	23.9	213	38	32.5	30.1	4
16	35	23.9	638	39	25	30.4	163
17	35	24.8	650	40	35	30.4	467
18	27.5	25.1	314	41	27.5	31.1	149
19	30	25.1	182	42	30	31.1	-3
20	32.5	25.1	151	43	32.5	31.1	6
21	25	25.8	269	44	25	31.7	195
22	27.5	26.4	194	45	35	31.7	293
23	30	26.4	337				

The modeled data were inserted into FPM model to calculate ETo and the results were calibrated through the equation of the relationship of fig. (3). after calibration, the *ETo_min*, *ETo_max* and *ETo_mean* of every month were extracted for the period of 35 years (1979-2014). The monthly *ETo_min*, *ETo_max* and *ETo_mean* of the 45 stations (represented in the table, 2) were used to producing the monthly *ETo_min*, *ETo_max* and *ETo_mean* maps based on *KSS* method. The conclusion of the methodology is represented in the next flowchart (fig., 4).

2.4 Kriging and interpolation

Kriging is a multi-steps process which uses separated and distributed points to create an estimated surface. It is a common method to interpolate the climate data and other environmental phenomena which distributed gradually [18].

It is the recommended geo-statistical method for producing weather maps. The general formula is:-

$$Z(S_o) = \sum_{i=1}^{N} \lambda_i \, Z(S_i) \qquad (2)$$

Where; $Z(s_i)$ is the measured value at the ith location, λ_i is an unknown weight for the measured value at the ith location which depends on the distance between the measured points, the prediction location and on the overall spatial arrangement of the measured points, s_o is the prediction location, N is the number of measured values.
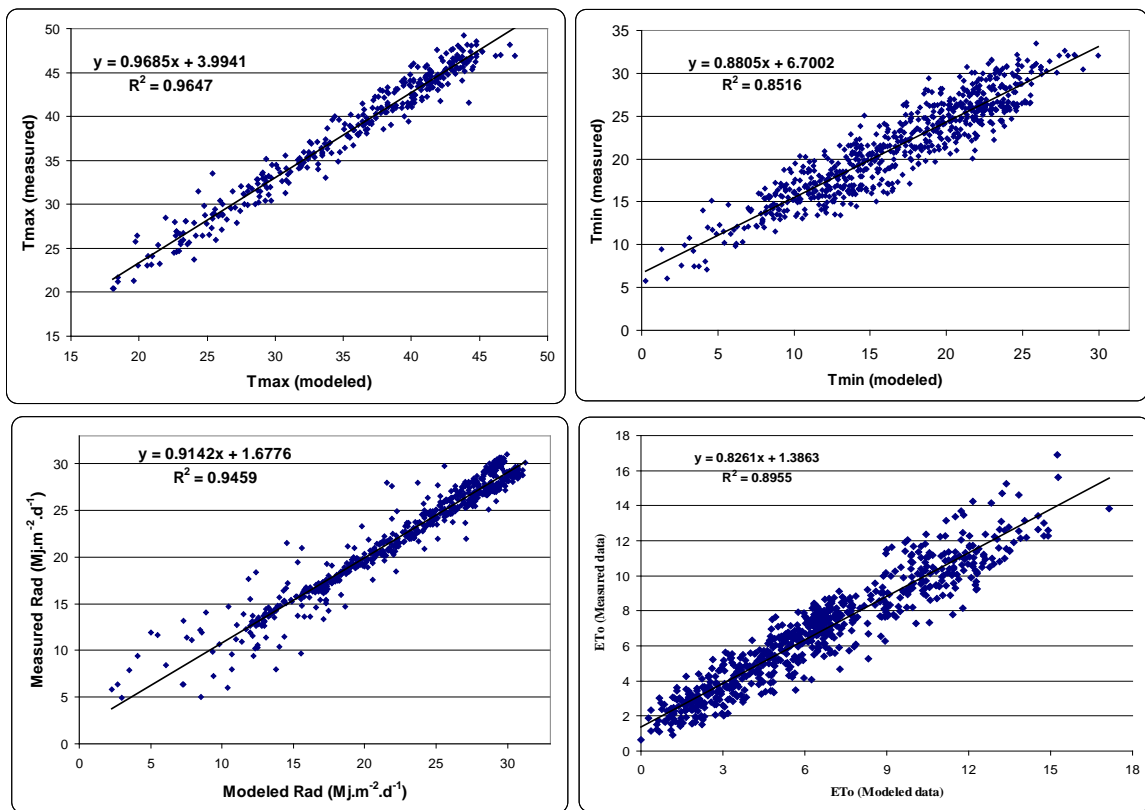
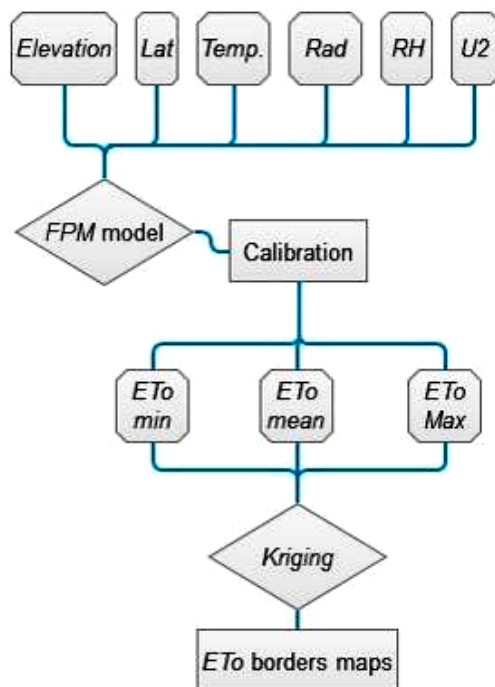Fig. 3 The relation between measured and modeled data

Fig. 4 Flowchart explains the processes of producing *ETo* borders maps

3. RESULTS AND DISCUSSION

ETo was estimated and calibrated, then the monthly average was calculated for every station during the period from 1979 to 2014. The minimum value of monthly *ETo* (*ETo_min*) was chosen for every station to represent the *ETo_min* border. The values of *ETo_min* for all stations are not in the same year. The results of *ETo_min* have been distributed according to time and space (month and station). For example; in a station, the value of *ETo_min* in January is not like *ETo_min* value in the rest of the stations in the same month. In the same time, *ETo_min* of January is not in the same year of *ETo_min* in the same station for February.

Monthly *ETo_min* and *ETo_Max* maps (Fig., 5 and 6) produced according to *KSS* method to represent the minimum and maximum borders maps of *ETo* for Egypt. The *ETo_min* values affected with decreasing of air temperature, solar radiation (sun hours), and wind speed besides increasing of *RH* and the opposite with *ETo_Max* [20-22].

The minimum border varied from 1.6 *mm/day* to about 11 *mm/day* according to location and time, while the maximum border varied from 3.6 *mm/day* to 13.2 *mm/day* according to location and time. The results are compatible with [4 and 13] where they calculated the *ETo* for deferent regions inside Egypt using *FPM* and Hargreaves methods.

There was overestimation for results of *ETo* based on Hargreaves than *FPM* method but after calibration with FPM, results will be close to ±0.5 mm/day. Results of *FPM* method are acceptable for most regions in the world because of it depend on multi-weather parameters, which cover all climate types.
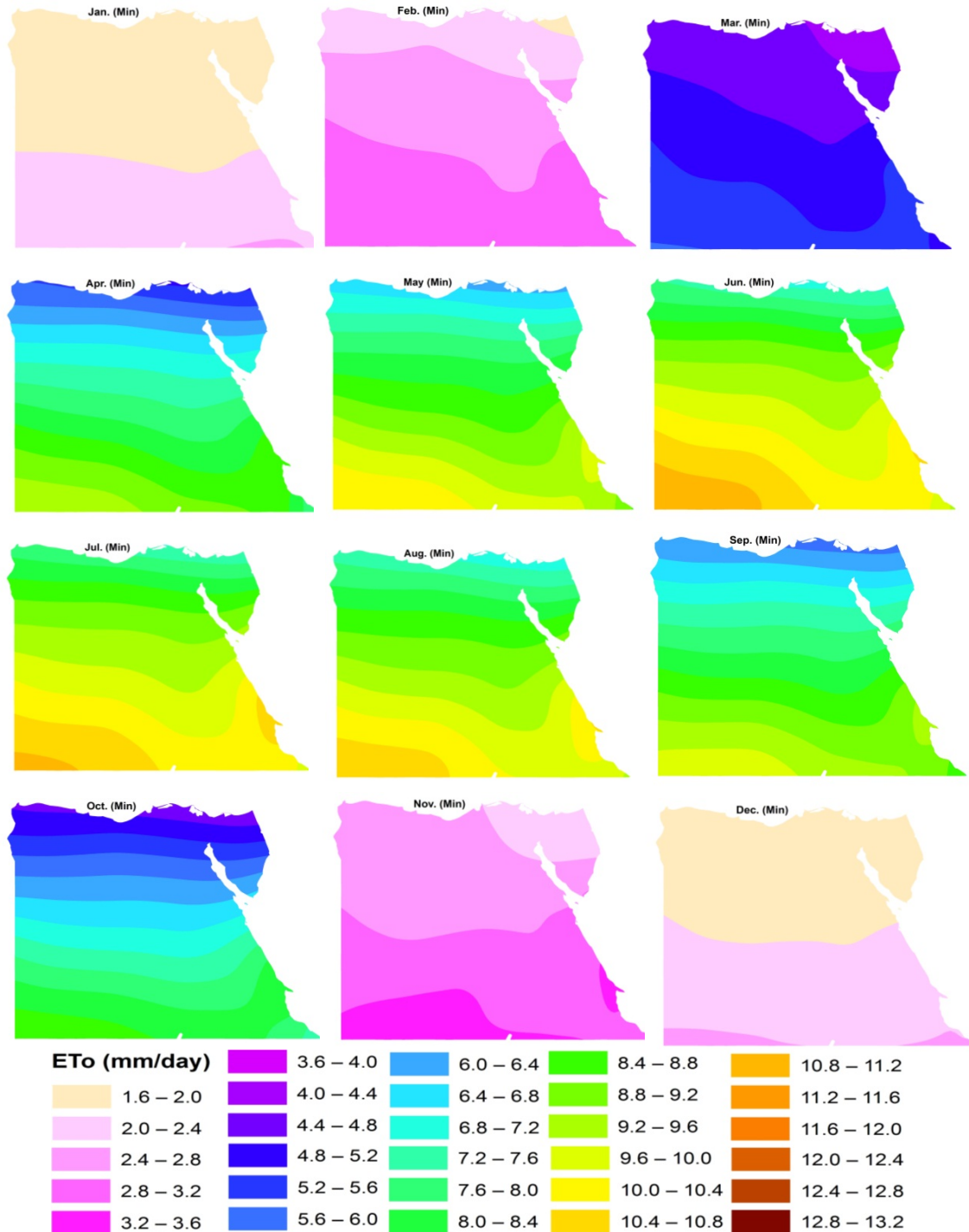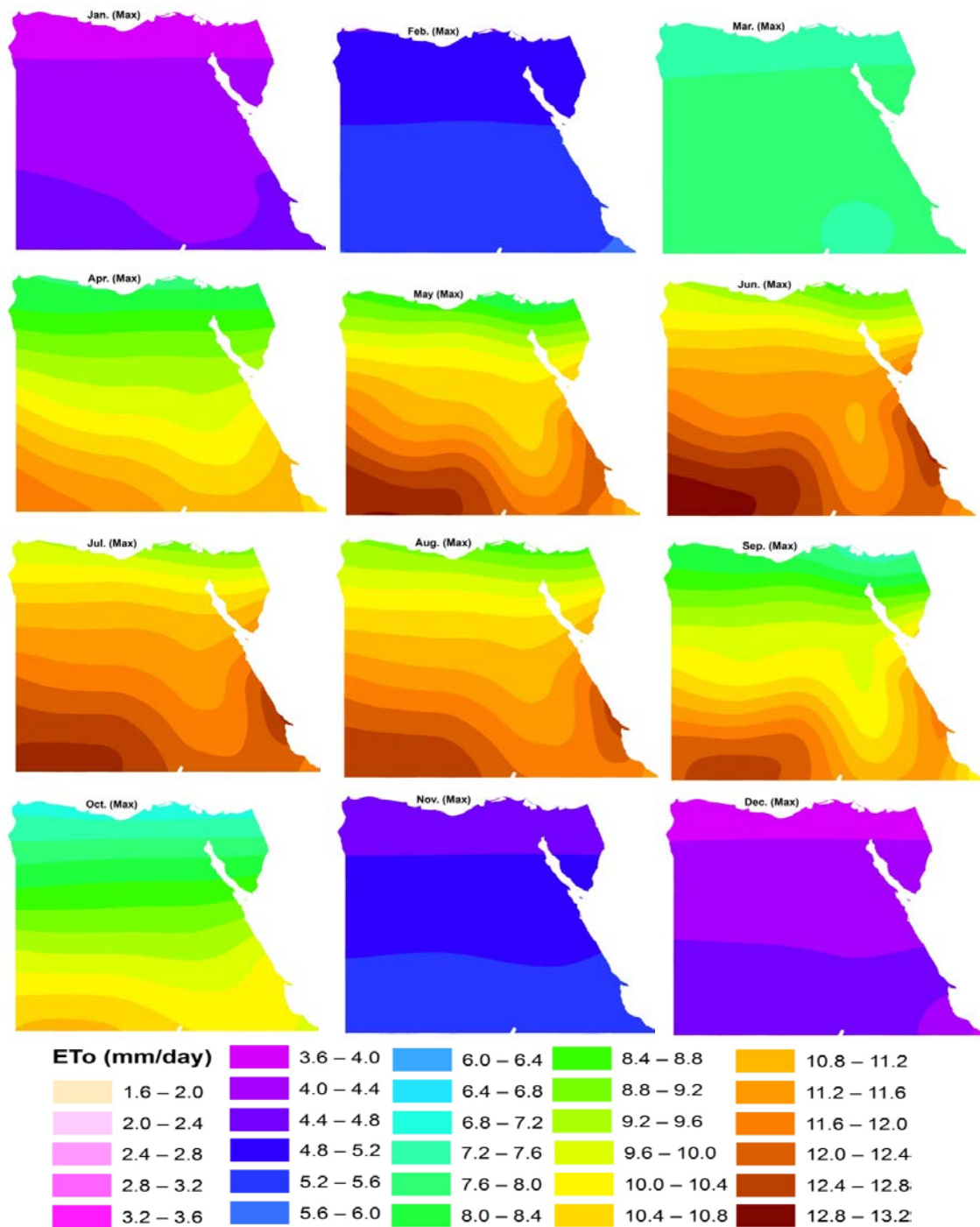

Fig. 5 The monthly *ETo_min* borders maps of Egypt

ETo (mm/day)			
3.6 − 4.0	6.0 − 6.4	8.4 − 8.8	10.8 − 11.2
1.6 − 2.0	4.0 − 4.4	8.8 − 9.2	11.2 − 11.6
2.0 − 2.4	4.4 − 4.8	9.2 − 9.6	11.6 − 12.0
2.4 − 2.8	4.8 − 5.2	9.6 − 10.0	12.0 − 12.4
2.8 − 3.2	5.2 − 5.6	10.0 − 10.4	12.4 − 12.8
3.2 − 3.6	5.6 − 6.0	10.4 − 10.8	12.8 − 13.2

Fig. 6 The monthly *ETo_Max* borders maps of Egypt

Monthly *ETo_mean* maps (Fig., 7) produced according to *KSS* method to represent the average *ETo* maps of Egypt. The *ETo_mean* maps are recommended for normal cases but upper (*ETo_Max*) and lower (*ETo_min*) borders recommended in the hottest and coldest years respectively. In the southern part of Egypt, the *ETo* is always higher than northern part, where the air

temperature and radiation are higher than the northern part. On the other hand, the *RH* is lower than the northern part.

The relation between modeled and predicted data through kriging was good where the average of R^2 was high as 0.87 and the average of standard error between measured and predicted was 0.09.
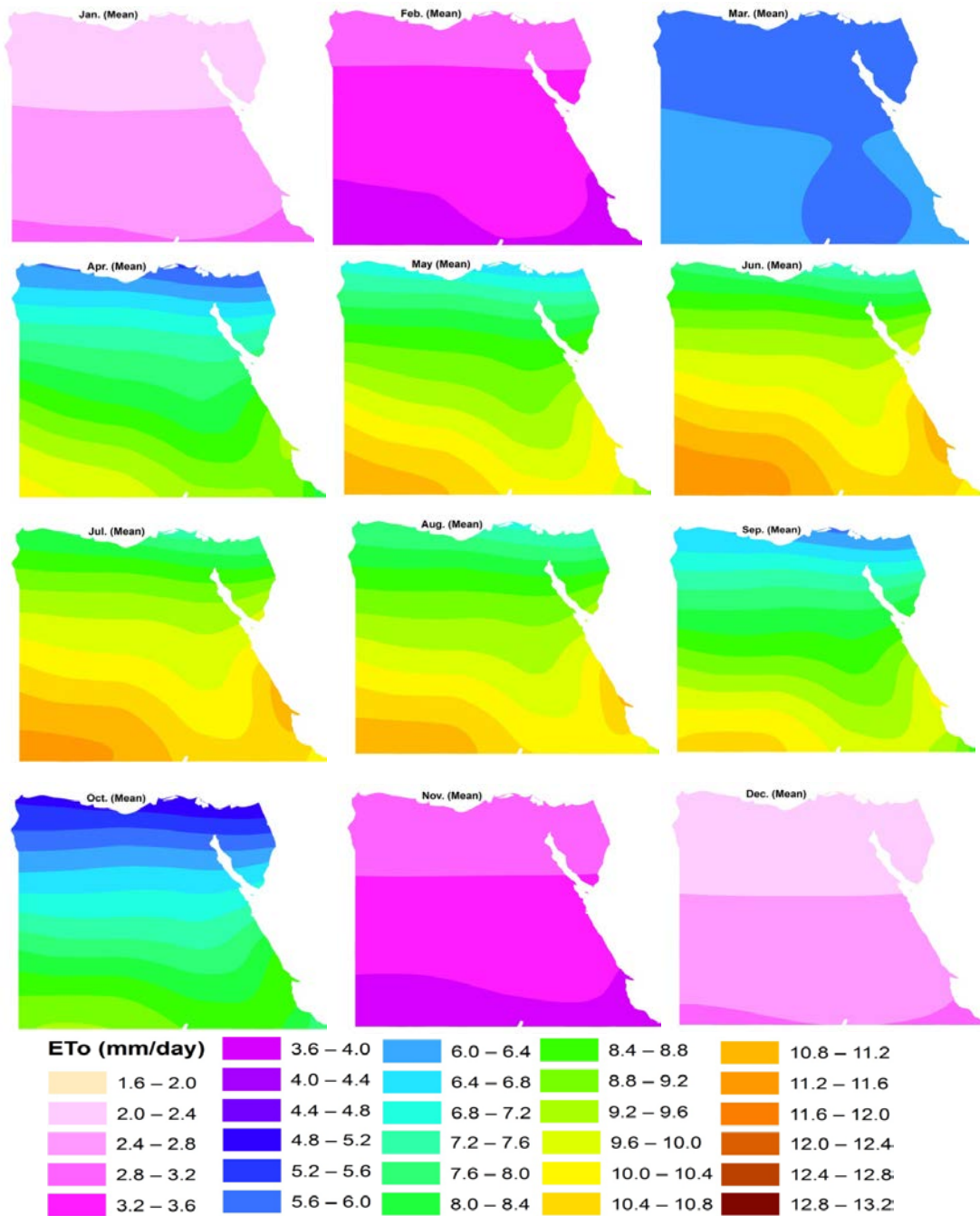
6

ETo (mm/day)			
1.6 – 2.0	4.0 – 4.4	6.4 – 6.8	8.8 – 9.2	11.2 – 11.6
2.0 – 2.4	4.4 – 4.8	6.8 – 7.2	9.2 – 9.6	11.6 – 12.0
2.4 – 2.8	4.8 – 5.2	7.2 – 7.6	9.6 – 10.0	12.0 – 12.4
2.8 – 3.2	5.2 – 5.6	7.6 – 8.0	10.0 – 10.4	12.4 – 12.8
3.2 – 3.6	5.6 – 6.0	8.0 – 8.4	10.4 – 10.8	12.8 – 13.2
3.6 – 4.0	6.0 – 6.4	8.4 – 8.8	10.8 – 11.2	

Fig. 7 The monthly *ETo_mean* maps of Egypt

4. CONCLUSION

Based on *ETo* maps of Egypt, the northern part is better than the southern part in terms of water consumption, where the northern part did not exceed 10 *mm/day* but the southern part exceed 13 *mm/day*. We recommend that the northern part is better for expanding the agricultural land as a first priority. Modeled data is very useful in case lack of data but validation and calibration are necessary. *KSS* is a powerful method to represent gradient environmental parameters and nature phenomena.

5. ACKNOWLEDGEMENTS

6. REFERENCES

[1] Egyptian ministry of water resources and irrigation, Water Scarcity in Egypt: The Urgent Need for Regional Cooperation among the Nile Basin Countries Report, 2014, pp. 5.

[2] Omar, M.M and Moussa, A.M.A. Water management in Egypt for facing the future challenges, Journal of Advanced Research, 7(3), 2016, pp. 403-412.

[3] Omar, M.M. Evaluation of actions for better water supply and demand management in Fayoum, Egypt using RIBASIM, Water Science, 27(54), 2013, pp. 78-90

[4] El-Shirbeny, M.A, Ali, A.M, Saleh, N.H. Crop Water Requirements in Egypt Using Remote Sensing Techniques. Journal of Agri. Chemistry and Enviro., 3, 2014, PP. 57-65.

[5] Petropoulos, G.P, Ireland, G, Lamine, S, Griffiths, H.M, Nicolas, N, Anagnostopoulos, V, North, M.R, Srivastava, P.K, Georgopoulou, H. Operational ET estimates from SEVIRI in support of sustainable water management, International Journal of Applied Earth Obs. and Geo-information, 49, 2016, pp. 175-187.

[6] Zhao, W, Liu, B, Chang, X, Yang, Q, Yang, Y, Liu, Z, Cleverly, J, Eamus, D. ET partitioning, stomatal conductance, and components of the water balance: A special case of a desert ecosystem in China, Journal of Hydrology, 538, 2016, pp. 374-386.

[7] Tillman, F.D, Wiele, S.M, Pool, D.R. A comparison of estimates of basin-scale soil-moisture evapotranspiration and estimates of riparian ground water evapotranspiration with implications for water budgets in the Verde Valley, Central Arizona, USA, Journal of Arid Environments, 124, 2016, pp. 278-291.

[8] Mansouri, Z, and Menani, M.R. Assessment of the water needs of apricot and olive crops under arid climatic conditions: case study of tinibaouine region (northeast of Algeria), Int. Journal of GEOMATE, 12(30), 2017, pp.46-52.

[9] Kageyama, S, Ikeda, S.T.M, and Ii, H. Water balance analysis considering runoff of ungauged catchments in iwaki river basin, northern japan, International Journal of GEOMATE, 9 (17), 2015, pp. 1434-1440.

[10] El-Shirbeny, M.A, Ali, A.M, Rashash, A, Badr M.A. Wheat Yield Response to Water Deficit under Central Pivot Irrigation System Using Remote Sensing Techniques, World Journal of Eng. and Tech., 3, 2015, pp. 65-72

[11] El-Shirbeny, M.A, Saleh, N.H, Ali, A.M. Estimation of Potential Crop ET Using Remote Sensing Techniques, Proce. of the 10th Inter. Conf. of AARSE, 2014, pp. 460-468.

[12] El-Shirbeny M.A, Alsersy M.A.M, Saleh N.H, Abu-Taleb K.A. Changes in irrigation water consumption in the Nile Delta of Egypt assessed by remote sensing, Arabian Journal of Geosciences, 8, 2015, pp. 10509–10519.

[13] El-Shirbeny, M.A, Abdellatif, B, Ali, A.M, Saleh, N.H. Evaluation of Hargreaves based on remote sensing method to estimate potential crop evapotranspiration, International Journal of GEOMATE, 11(23), 2016, PP. 2143-2149.

[14] Allen, R.G, Pereira, L.S, Raes, D, Smith, M. Crop ET-Guidelines for computing crop water requirements, FAO Irrigation and drainage paper 56, FAO, Rome, 1998.

[15] Xu, j, Liu, x, Yang, S, Qi, Z, Wang, Y. Modeling rice ET under water-saving irrigation by calibrating canopy resistance model parameters in the Penman-Monteith equation, Agri. Water Manag., 182, 2017, PP. 55-66

[16] Feng, Y, Jia, Y, Cui, N, Zhao, L, Li, C, Gong, D. Calibration of Hargreaves model for reference ET estimation in Sichuan basin of southwest China, Agri. Water Manag., 181, 2017, PP. 1-9.

[17] Ganji, H, Kajisa, T, Kondo, M, Ito, R, Rostami, B. Re- examining the validity of reference evapotranspiration estimation in Herat, Afghanistan, International Journal of GEOMATE, 12(30), 2017, pp. 61-68.

[18] Boer, E., Beurs, K., Hartkamp, A. Kriging and thin plate splines for mapping climate variables, Int. Journa of Applied Earth Obs. and Geoinf., 3(2), 2001, pp. 146-154

[19] Mujahed, M.M. Energy sources in Egypt and the prospects of development (In Arabic), Academic Library, 2014, p.51.

[20] Wang, Z, Xie, P, Lai, C, Chen, X, Wu, X, Zeng, Z, Li, J. Spatiotemporal variability of reference evapotranspiration and contributing climatic factors in China during 1961–2013, Journal of Hydrology, 544, 2017, pp.97-108

[21] Yang, Y, Cui, Y, Luo, Y, Lyu, X, Traore, S, Khan, S, Wang, W. Short-term forecasting of daily reference ET using the Penman-Monteith model and public weather forecasts, Agri. Water Manag., 177, 2016, pp. 329-339

[22] Djaman, K, Tabari, H, Balde, A.B, Diop, L, Futakuchi, K, Irmak, S. Analyses, calibration and validation of ET models to predict grass-reference ET in the Senegal river delta, Journal of Hydrology: Regional Studies, 8, 2016, pp. 82-94.